Published in Inorganica Chimica Acta 359, issue 10, 3297-3305, 2006
which should be used for any reference to this work

Dinuclear iron, ruthenium and cobalt complexes containing 1,4-dimethyl-1,4,7-triazacyclononane ligands as well as carboxylato and oxo or hydroxo bridges

Vladimir B. Romakh, Bruno Therrien, Gaël Labat, Helen Stoekli-Evans, Georgiy B. Shul'pin, Georg Süss-Fink *

Institut de Chimie, Université de Neuchâtel, Case postale 158, CH-2009 Neuchâtel, Switzerland

Abstract

The reaction of 1,4-dimethyl-1,4,7-triazacyclononane (L–Me_2) with $FeSO_4 \cdot 7H_2O$ in aqueous ethanol gives, in the presence of sodium carboxylates, hydrogen peroxide, sodium hydroxide and KPF_6, the dinuclear Fe(III)–Fe(III) complex cations $[(L–Me_2)_2Fe_2(O)(OOCR)_2]^{2+}$ (R = H: **1**, R = CH_3: **2**, R = C_6H_5: **3**), which crystallise as the hexafluorophosphate salts. The corresponding reaction with $RuCl_3 \cdot nH_2O$ does not work, however, the analogous Ru(III)–Ru(III) complex $[(L–Me_2)_2Ru_2(O)(OOCCH_3)_2]^{2+}$ (**5**) can be synthesised by reacting $Ru(dmso)_4Cl_2$ with L–Me_2, HCl and air in refluxing ethanol, followed by addition of sodium acetate, the mononuclear intermediate $(L–Me_2)RuCl_3 \cdot H_2O$ (**4**) being also isolated and characterised. The reaction of L–Me_2, sodium acetate, hydrogen peroxide and triethylamine with $CoCl_2 \cdot 6H_2O$ in acetonitrile yields, however, the hydroxo-bridged Co(III)–Co(III) complex $[(L–Me_2)_2Co_2(OH)(OOCCH_3)_2]^{3+}$ (**6**). The molecular structures of **2**, **5** and **6**, solved by single-crystal X-ray structure analyses of the hexafluorophosphate salts, reveal for the orange crystals of [**2**][PF_6]$_2$ a Fe–Fe distance of 3.104(1) Å, for the purple crystals of [**5**][PF_6]$_2$ a Ru–Ru distance of 3.230(1) Å, and for the violet crystals of [**6**][PF_6]$_3 \cdot (CH_3)_2CO$ a Co–Co distance of 3.358(1) Å. All six complexes show catalytic activity for the oxidation of isopropanol with hydrogen peroxide in water to give acetone in the presence of ascorbic acid as co-catalyst.

Keywords: 1,4-dimethyl-1,4,7-triazacyclononane ligand; Oxidation; Hydrogen peroxide; Iron; Ruthenium; Cobalt

1. Introduction

Iron complexes containing macrocyclic ligands with three nitrogen-donor atoms as well as carboxylato and oxo bridges have found much interest as model complexes relevant to biocatalysis [1,2]. In particular, the coordination chemistry of 1,4,7-triazacyclononane and its derivatives has been pioneered by Wieghardt in the 1980s. Thus, 1,4,7-triazacyclononane (L) was found to react with iron(III) chloride hexahydrate and ammonium acetate to give the dinuclear Fe(III)–Fe(III) complex $[L_2Fe_2(O)(OOCCH_3)_2]^{2+}$ [3], which has been described as a model for the active centre of hemerythrin. Starting from 1,4,7-trimethyl-1,4,7-triazacyclononane (L–Me_3), iron(II) perchlorate hexahydrate and iron(III) chloride hexahydrate, the dinuclear Fe(II)–Fe(II) $[(L–Me_3)_2Fe_2(OH)(OOCCH_3)_2]^{+}$ and the corresponding Fe(III)–Fe(III) $[(L–Me_3)_2Fe_2(O)(OOCCH_3)_2]^{2+}$ are accessible [4], which have been studied by Lippard as functional models for methane monooxygenase [5] (see Scheme 1). A mixed-valent Fe(III)–Fe(IV) complex $[L_2Fe_2(O)(OOCCH_3)_2]^{3+}$ can be generated electrochemically or chemically with aminyl radical cations at −30 °C in acetonitrile [6].

In the case of ruthenium, using 1,4,7-trimethyl-1,4,7-triazacyclononane as a tripodal ligand, even the Ru(IV)

* Corresponding author.
E-mail addresses: bruno.therrien@unine.ch (B. Therrien), georg.suess-fink@unine.ch (G. Süss-Fink).

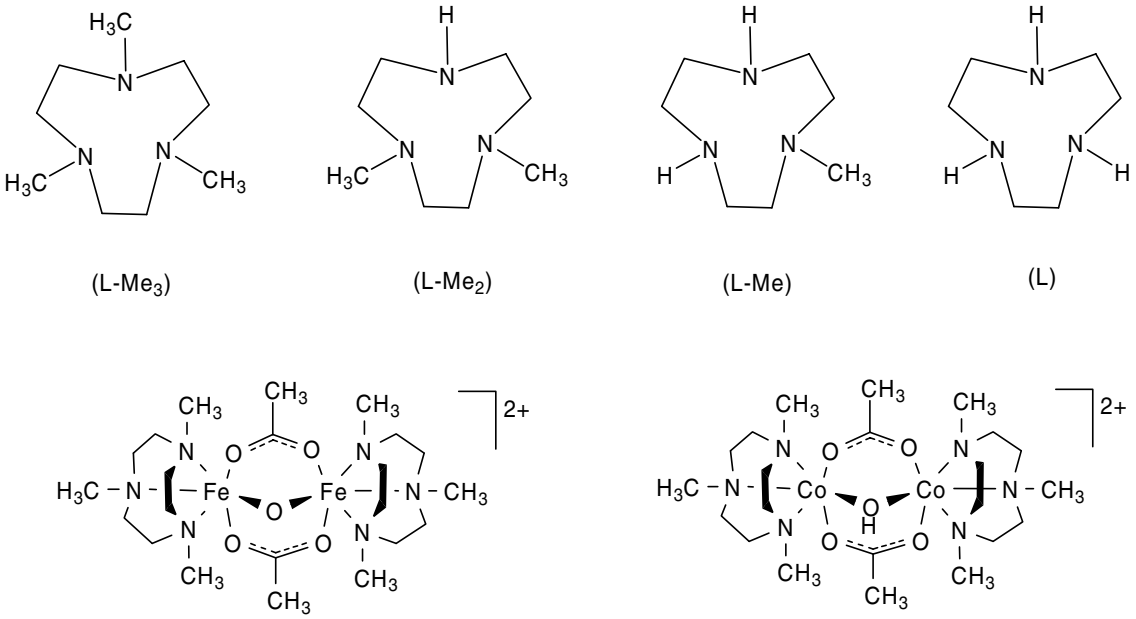

Scheme 1. Triazacyclononane ligands, dinuclear iron and cobalt complexes containing the trimethyl derivative.

oxidation state of the metal centre is accessible. Thus, reaction of the dimethylsulfoxide complex $RuCl_2(dmso)_4$ with 1,4,7-trimethyl-1,4,7-triazacyclononane in ethanol, followed by treatment with HCl in air, yields $(L–Me_3)RuCl_3 \cdot H_2O$, which can be converted in the presence of carboxylate anions into dinuclear Ru(III)–Ru(III) (μ-oxo)-bis(μ-carboxylato) complexes [7]. In the case of sodium acetate, two Ru(III)–Ru(III) complexes $[(L–Me_3)_2Ru_2(OH)(OOCCH_3)_2]^{3+}$ and $[(L–Me_3)_2Ru_2(O)(OOCCH_3)_2]^{2+}$ can be isolated; the latter one can be oxidised into the Ru(III)–Ru(IV) complex $[(L–Me_3)_2Ru_2(O)(OOCCH_3)_2]^{3+}$ [7], or converted into the Ru(II)–Ru(III), Ru(III)–Ru(III) and Ru(IV)–Ru(IV) complexes $[(L–Me_3)_2Ru_2(OH)_3]^{2+}$, $[(L–Me_3)_2Ru_2(OH)_3]^{3+}$ and $[(L–Me_3)_2Ru_2(O)_3]^{2+}$ [8], respectively.

Dinuclear carboxylato-bridged complexes of cobalt are surprisingly rare, considering the enormous structural variety of such compounds. A full series of dinuclear Co(II)–Co(II), Co(II)–Co(III) and Co(III)–Co(III) di-μ-acetato complexes, containing 1,4,7-trimethyl-1,4,7-triazacyclononane, $[(L–Me_3)_2Co_2(OH)(OOCCH_3)_2]^{+}$, $[(L–Me_3)_2Co_2(OH)(OOCCH_3)_2]^{2+}$ and $[(L–Me_3)_2Co_2(OH)(OOCCH_3)_2]^{3+}$, has been reported by Wieghardt [9].

After the discovery of the catalytic activity of iron(III) complexes containing 1,4,7-trimethyl-1,4,7-triazacyclononane for low-temperature bleaching [10], the catalytic oxidation potential of this type of complexes has been demonstrated for the oxidation of phosphines [11] and sulfides [12] with dioxygen and benzylic groups with hydrogen peroxide [13]. We showed that the presence of pyrazine-2-carboxylic acid strongly increases the catalytic oxidation potential of the dinuclear Fe(III)–Fe(III) complex $[L_2Fe_2(O)(OOCCH_3)_2]^{2+}$ [14], so that even alkanes, including ethane and methane, could be oxidised with hydrogen peroxide in acetonitrile. The mononuclear ruthenium(III) complex $[(L–Me_3)Ru(OOCCF_3)_3]$ has been reported as an effective catalyst for the epoxidation of alkenes [15] and for the oxidation of alcohols with *t*-butylhydroperoxide, under mild conditions [16].

Herein, we report a straight-forward synthesis for dinuclear Fe(III)–Fe(III) and Co(III)–Co(III) complexes containing $L–Me_2$ ligands as well as carboxylato and oxo or hydroxo bridges, as well as a synthetic route to the Ru(III)–Ru(III) analogue $[(L–Me_2)_2Ru_2(O)(OOCCH_3)_2]^{2+}$, all cations can be isolated as the hexafluorophosphate salts. The catalytic oxidation properties of these compounds are discussed.

2. Experimental

2.1. General remarks

All reactions were carried out by standard Schlenk techniques under nitrogen atmosphere. Organic solvents and bidistilled water were degassed and saturated with nitrogen prior to use. Infrared and UV/Vis spectra were recorded using Perkin–Elmer Spectrum One and UVICON-930 spectrophotometers, respectively. Microanalyses were performed by the Laboratory of Pharmaceutical Chemistry, University of Geneva (Switzerland) and the Laboratory of Organic Chemistry, ETH Zurich (Switzerland). The starting compound, 1,4-dimethyl-1,4,7-triazacyclononane ($L–Me_2$), was prepared according to the published method [17] and redistilled prior to use. The ruthenium(II) complex $RuCl_2(dmso)_4$ was synthesised by a procedure reported by Spencer and Wilkinson [18]. Iron(II) sulfate heptahydrate, iron(II) chloride, cobalt(II) chloride hexahydrate, sodium formate monohydrate, sodium acetate trihydrate, sodium

benzoate, potassium hexafluorophosphate, *p*-toluenesulfonic acid monohydrate, hydrogen peroxide (30 wt% solution in water), ascorbic acid, sodium hydroxide and triethylamine were purchased from Acros, Aldrich or Fluka and were used without further purification.

2.2. Syntheses

General procedure for $[(L–Me_2)_2Fe_2(O)(OOC–R)_2][PF_6]_2$: In a 50 mL Schlenk tube, a mixture of L–Me_2 (157.3 mg, 1.00 mmol) and *p*-toluenesulfonic acid monohydrate (190.2 mg, 1.00 mmol) was dissolved in 10 mL of 80% aqueous ethanol. To this clear light-yellow solution, solid $FeSO_4 \cdot 7H_2O$ (278 mg, 1.00 mmol) was added under vigorous stirring. The mixture was treated with ultrasound (10–15 min) and then stirred for half an hour. Then, KPF_6 (276 mg, 1.50 mmol) and the corresponding sodium carboxylate (**1**: $HCOONa \cdot H_2O$, 129 mg, 1.50 mmol; **2**: $CH_3COONa \cdot 3H_2O$, 204 mg, 1.50 mmol; **3**: C_6H_5COONa, 216 mg, 1.50 mmol) were added to the slurry. After stirring at 45 °C for 60 min, the suspension was cooled to 0 °C, before a freshly prepared aqueous solution (2 mL) of H_2O_2 (102 μL, 1.0 mmol) and NaOH (48 mg, 1.2 mmol) was added. Then the resulting orange suspension was stirred at 20 °C for 2 h. After filtration through celite and washing 2 times with 2 mL of water, the orange solid on the celite bed was recovered with acetone, purified on neutral aluminium oxide (eluent acetone/methanol 5:1) and isolated by evaporation of the solvent (0.05 mbar, 20 °C, 24 h). Single-crystals suitable for X-ray analysis were grown from an acetone solution, into which ether was allowed to slowly diffuse within 48 h.

*$[(L–Me_2)_2Fe_2(O)(OOCH)_2][PF_6][SO_4]_{0.5}$ (**[1][PF6]-[SO4]0.5**)*. Yield: 42–54%. UV–Vis (CH_3CN) λ_{max} (nm): 240 ($\varepsilon = 13\,800\ cm^{-1}\ mol^{-1}\ L$), 339 (7800), 474 (1100), 500 (sh), 698 (150). IR (KBr pellets) ν (cm^{-1}): 3331(m), 3263(m), 2908(s), 2871(s), 1624(s), 1566(vs), 1496(m), 1463(s), 1362(s), 1303(m), 1100(m), 1007(s), 840(vs), 750(s), 558(s), 491(m). *Anal*. Calc. for $C_{18}H_{40}F_6Fe_2N_6O_7P_1S_{0.5}$: C, 29.81; H, 5.56; N, 11.59. Found: C, 29.74; H, 5.68; N, 11.50%.

*$[(L–Me_2)_2Fe_2(O)(OOCCH_3)_2][PF_6]_2$ (**[2][PF6]2**)*. Yield: 52–61%. UV–Vis (CH_3CN) λ_{max} (nm): 230 ($\varepsilon = 14\,600\ cm^{-1}\ mol^{-1}\ L$), 341 (6700), 473 (1460), 516 (1100), 550 (sh), 748 (145). IR (KBr pellets) ν (cm^{-1}): 3332(s), 2991(m), 2951(m), 1554(s), 1495(m), 1463(s), 1425(s), 1097(m), 1028(s), 1007(s), 960(m), 839(vs), 725(s), 664(m), 558(s). *Anal*. Calc. for $C_{20}H_{44}F_{12}Fe_2N_6O_5P_2 \cdot 0.5(CH_3)_2CO$: C, 29.37; H, 5.39; N, 9.56. Found: C, 29.30; H, 5.34; N, 9.67%.

*$[(L–Me_2)_2Fe_2(O)(OOCC_6H_5)_2][PF_6]_2$ (**[3][PF6]2**)*. Yield: 75%. UV–Vis (CH_3CN) λ_{max} (nm): 237 ($\varepsilon = 27\,800\ cm^{-1}\ mol^{-1}\ L$), 338 (8200), 476 (1500), 517 (1140), 550 (sh), 745 (140). IR (KBr pellets) ν (cm^{-1}): 3329(m), 2981(m), 2929(m), 1593(m), 1538(s), 1494(m), 1463(s), 1400(vs), 1178(m), 1096(m), 1027(m), 1007(s), 961(m), 839(vs), 724(s), 677(m), 558(s), 471(m). *Anal*. Calc. for $C_{30}H_{48}F_{12}Fe_2N_6O_5P_2 \cdot 0.5(CH_3)_2CO$: C, 37.71; H, 5.12; N, 8.38. Found: C, 37.74; H, 5.32; N, 8.73%.

*$(L–Me_2)RuCl_3 \cdot H_2O$ (**4**)*. A procedure reported by Wieghardt for $(L–Me_3)RuCl_3 \cdot H_2O$ [8] was used with minor modifications. In a 50 mL Schlenk tube, a mixture of L–Me_2 (315 mg, 2.00 mmol) and $RuCl_2(dmso)_4$ (436 mg, 0.90 mmol) was suspended in 10 mL of absolute ethanol. The mixture was stirred at 60 °C for 30 min, until a clear brown-red solution was obtained, and then refluxed for 2 h. The solvent was removed by rotary evaporation, and the solid was refluxed in 37% HCl (10 mL) for 30 min in the presence of air. The brown-orange solution was evaporated and the solid was suspended in 5 mL of water. The orange microcrystalline product was filtered, washed with water, ethanol, ether and dried in vacuo.

*$(L–Me_2)RuCl_3 \cdot H_2O$ (**4**)*. Yield: 41%. UV–Vis (CH_3CN–H_2O) λ_{max} (nm): 229 ($\varepsilon = 6800\ cm^{-1}\ mol^{-1}\ L$), 295 (1250), 386 (2100). IR (KBr pellets) ν (cm^{-1}): 3391(vs), 3183(vs), 2992(m), 2925(s), 1915(m), 1632(s), 1489(m), 1449(vs), 1384(s), 1274(m), 1095(s), 1045(s), 998(s), 960(s), 826(s), 765(m), 744(m), 612(m), 519(m), 482(m), 436(m). *Anal*. Calc. for $C_8H_{19}Cl_3N_3Ru \cdot H_2O$: C, 25.11; H, 5.53; N, 10.98. Found: C, 25.27; H, 5.35; N, 10.94%.

*$[(L–Me_2)_2Ru_2(O)(OOCCH_3)_2][PF_6]_2$ (**[5][PF6]2**)*. In a 50 mL Schlenk tube, $(L–Me_2)RuCl_3 \cdot H_2O$ (120 mg, 0.31 mmol) was suspended in 7 mL of water and $CH_3COONa \cdot 3H_2O$ (422 mg, 3.10 mmol) was added. The mixture was refluxed for 30 min, until a clear deep-violet solution was obtained. To this hot solution, KPF_6 (350 mg, 1.90 mmol) dissolved in 5 mL of water was added and the final product precipitated after 12 h at 0 °C. The dark-violet microcrystalline solid was filtered, washed with water, ethanol, ether and dried in vacuo. Single X-ray quality crystals were grown from an acetone solution, into which ether was allowed to slowly diffuse within 48 h.

*$[(L–Me_2)_2Ru_2(O)(OOCCH_3)_2][PF_6]_2$ (**[5][PF6]2**)*. Yield: 73%. UV–Vis (CH_3CN) λ_{max} (nm): 233 ($\varepsilon = 10\,200\ cm^{-1}\ mol^{-1}\ L$), 279 (8900), 325 (sh), 538 (6700). IR (KBr pellets) ν (cm^{-1}): 3435(m), 3310(s), 2933(m), 1631(m), 1559(s), 1464(s), 1428(s), 1100(m), 1037(m), 1006(m), 842(vs), 766(m), 684(m), 558(s), 520(m), 471(m), 440(m). *Anal*. Calc. for $C_{20}H_{44}F_{12}N_6O_5P_2Ru_2 \cdot 2H_2O$: C, 24.59; H, 4.95; N, 8.60. Found: C, 24.55; H, 4.42; N, 8.34%.

*$[(L–Me_2)_2Co_2(OH)(OOCCH_3)_2][PF_6]_3$ (**[6][PF6]3**)*. In a 50 mL Schlenk tube, a mixture of L–Me_2 (157.3 mg, 1.00 mmol) and *p*-toluenesulfonic acid monohydrate (190.2 mg, 1.00 mmol) was dissolved in 15 mL of acetonitrile. To this clear light-yellow solution, solid $CoCl_2 \cdot 6H_2O$ (238 mg, 1.00 mmol) was added under vigorous stirring. The mixture was treated with ultrasound (10–15 min), before KPF_6 (276 mg, 1.50 mmol) and $CH_3COONa \cdot 3H_2O$ (204 mg, 1.50 mmol) were added to the deep blue suspension. After stirring at 60 °C for 20 min, followed by cooling to 0 °C, an acetonitrile solution containing H_2O_2 (102 μL, 1.0 mmol) and triethylamine (278 μL, 2.0 mmol) was added. Then the pink-brown suspension was stirred at

20 °C for 2 h. After filtration through celite and washing with 2 mL of acetone, the filtrate was evaporated in vacuo. The product was resuspended in water (2 mL), filtered, washed with water, ethanol, ether and dried under vacuum. Single-crystals suitable for X-ray analysis were grown from an acetone solution, into which ether was allowed to slowly diffuse within 48 h.

*[(L–Me$_2$)$_2$Co$_2$(OH)(OOCCH$_3$)$_2$][PF$_6$]$_3$ ([**6**][PF$_6$]$_3$).* Yield: 40%. UV–Vis (CH_3CN) λ_{max} (nm): 535 (ε = 260 cm^{-1} mol^{-1} L), 330 (sh). IR (KBr pellets) ν (cm^{-1}): 3568(m), 3436(m), 3249(m), 2958(m), 1688(s), 1590(vs), 1502(m), 1452(s), 1080(m), 1046(m), 1011(m), 981(m), 841(vs), 697(m), 558(s). *Anal.* Calc. for $C_{20}H_{45}F_{18}Co_2N_6O_5P_3 \cdot (CH_3)_2CO \cdot H_2O$: C, 25.62; H, 4.95; N, 7.79. Found: C, 25.55; H, 4.90; N, 7.95%.

2.3. X-ray crystallographic studies

Single-crystals of [**2**][PF$_6$]$_2$, [**5**][PF$_6$]$_2$ and [**6**][PF$_6$]$_3 \cdot (CH_3)_2CO$ were mounted on a Stoe Image Plate Diffraction system equipped with a ϕ circle goniometer, using Mo Kα graphite monochromated radiation ($\lambda = 0.71073$ Å) with ϕ range 0–200°, increment of 1.5°, 1.4° and 1.5°, respectively, $D_{max} - D_{min} = 12.45 - 0.81$ Å. The structures were solved by direct methods using the program SHELXS-97 [19]. Refinement and all further calculations were carried out using SHELXL-97 [20]. In all compounds, the hydrogen atoms have been included in calculated positions and treated as riding atoms using the SHELXL default parameters. All non-H atoms were refined anisotropically, using weighted full-matrix least-square on F^2. In [**2**][PF$_6$]$_2$, a semi-empirical absorption correction was applied using MULABS (PLATON03 [21], $T_{min} = 0.776$, $T_{max} = 0.961$). Crystallographic details are summarised in Table 1. Figs. 1–3 were drawn with ORTEP [22] and Fig. 4 with MERCURY [23].

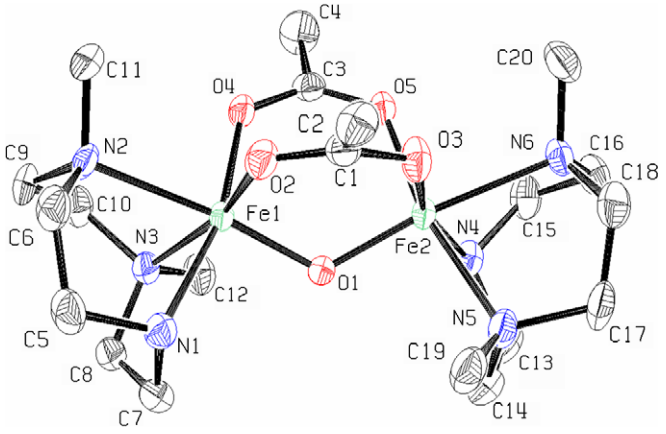

Fig. 1. The molecular structure of $[(L–Me_2)_2Fe_2(O)(OOCCH_3)_2]^{2+}$ (**2**): displacement ellipsoids are drawn at the 50% probability level; hydrogen atoms and hexafluorophosphate molecules are omitted for clarity. Selected bond lengths (Å) and angles (°): Fe(1)–Fe(2) 3.1038(11), Fe(1)–N(1) 2.151(5), Fe(1)–N(2) 2.243(5), Fe(1)–N(3) 2.193(5), Fe(2)–N(4) 2.159(5), Fe(2)–N(5) 2.197(5), Fe(2)–N(6) 2.252(5), Fe(1)–O(1) 1.788(4), Fe(2)–O(1) 1.796(4), Fe(1)–O(2) 2.027(4), Fe(1)–O(4) 2.023(4), Fe(2)–O(3) 2.018(4), Fe(2)–O(5) 2.040(4); Fe(1)–O(1)–Fe(2) 120.0(2), O(2)–C(1)–O(3) 124.6(6), O(4)–C(3)–O(5) 125.0(6).

2.4. Catalytic runs

The oxidation of isopropanol was carried out in air in thermostated cylindrical pyrex vessels with vigorous stir-

Table 1
Crystallographic and selected experimental data for [**2**][PF$_6$]$_2$, [**5**][PF$_6$]$_2$ and [**6**][PF$_6$]$_3 \cdot (CH_3)_2CO$

	[**2**][PF$_6$]$_2$	[**5**][PF$_6$]$_2$	[**6**][PF$_6$]$_3 \cdot (CH_3)_2CO$
Chemical formula	$C_{20}H_{44}F_{12}Fe_2N_6O_5P_2$	$C_{20}H_{44}F_{12}N_6O_5P_2Ru_2$	$C_{23}H_{51}Co_2F_{18}N_6O_6P_3$
Formula weight	850.25	940.69	1060.47
Crystal system	monoclinic	orthorhombic	triclinic
Space group	$P2_1/n$	*Cmca*	$P\bar{1}$
Crystal colour and shape	orange block	purple plate	violet block
Crystal size	0.4 × 0.3 × 0.2	0.34 × 0.22 × 0.08	0.37 × 0.20 × 0.12
a (Å)	14.410(2)	33.806(7)	10.976(2)
b (Å)	16.547(2)	13.853(3)	11.246(2)
c (Å)	15.341(3)	15.199(3)	16.389(3)
α (°)			104.67(1)
β (°)	116.026(11)		92.67(1)
γ (°)			95.49(1)
V (Å^3)	3287.1(8)	7118(3)	1942.9(6)
Z	4	8	2
T (K)	173(2)	203(2)	203(2)
D_{calc} (g cm^{-3})	1.718	1.756	1.813
μ (mm^{-1})	1.090	1.040	1.110
Scan range (°)	$1.62 < \theta < 25.70$	$2.08 < \theta < 26.00$	$1.29 < 2\theta < 25.25$
Unique reflections	6238	3281	6932
Reflections used [$I > 2\sigma(I)$]	4185	1344	3923
R_{int}	0.1139	0.0904	0.1520
Final R indices [$I > 2\sigma(I)$]	$R_1 = 0.0692$, $wR_2 = 0.1610$	$R_1 = 0.0474$, $wR_2 = 0.1095$	$R_1 = 0.0683$, $wR_2 = 0.1532$
R indices (all data)	$R_1 = 0.1091$, $wR_2 = 0.1774$	$R_1 = 0.0890$, $wR_2 = 0.1491$	$R_1 = 0.1228$, $wR_2 = 0.1765$
Goodness-of-fit	1.042	0.793	0.929
Maximum, minimum $\Delta\rho$ (e Å^{-3})	0.964, −1.352	0.448, −0.423	0.552, −1.264

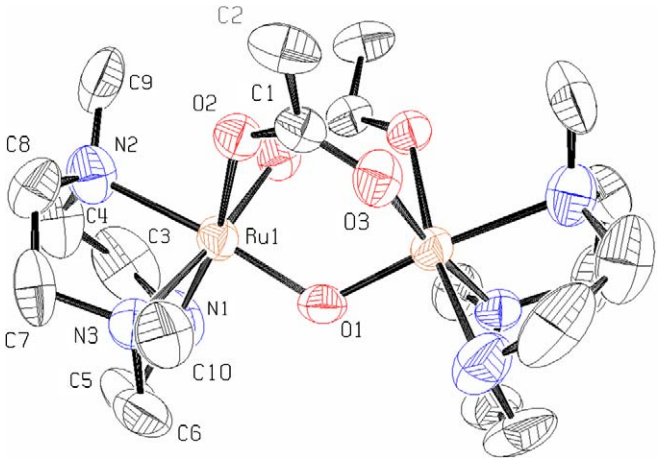

Fig. 2. The molecular structure of $[(L–Me_2)_2Ru_2(O)(OOCCH_3)_2]^{2+}$ (**5**): displacement ellipsoids are drawn at the 50% probability level; hydrogen atoms and hexafluorophosphate molecules are omitted for clarity. Selected bond lengths (Å) and angles (°): Ru(1)–Ru(1)^{i} 3.2299(12), Ru(1)–N(1) 2.068(6), Ru(1)–N(2) 2.172(7), Ru(1)–N(3) 2.092(8), Ru(1)–O(1) 1.850(4), Ru(1)–O(2) 2.084(5), Ru(1)^{i}–O(3) 2.079(6); Ru(1)–O(1)–Ru(1)^{i} 121.6(4), O(2)–C(1)–O(3) 124.8(7). ^{i} x, $-y$, $1-z$.

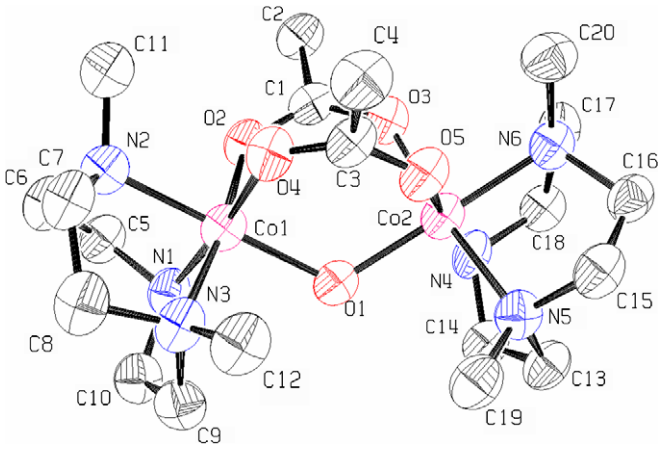

Fig. 3. The molecular structure of $[(L–Me_2)_2Co_2(OH)(OOCCH_3)_2]^{3+}$ (**6**): displacement ellipsoids are drawn at the 50% probability level; hydrogen atoms, acetone and hexafluorophosphate molecules are omitted for clarity. Selected bond lengths (Å) and angles (°): Co(1)–Co(2) 3.3584(14), Co(1)–N(1) 1.930(5), Co(1)–N(2) 1.987(6), Co(1)–N(3) 1.969(6), Co(2)–N(4) 1.939(5), Co(2)–N(5) 1.968(5), Co(2)–N(6) 1.989(6), Co(1)–O(1) 1.936(4), Co(2)–O(1) 1.927(4), Co(1)–O(2) 1.863(4), Co(1)–O(4) 1.894(4), Co(2)–O(3) 1.912(4), Co(2)–O(5) 1.895(4); Co(1)–O(1)–Co(2) 120.8(2), O(2)–C(1)–O(3) 125.8(6), O(4)–C(3)–O(5) 125.9(6).

ring at 20.0 °C. The total volume of the reaction solution was 10 mL. In a typical experiment, 512 μL of hydrogen peroxide (30% aqueous solution, 0.50 M) was added to a mixture containing the catalyst (1.0×10^{-4} M), ascorbic acid (0.01 M) and isopropanol (153 μL, 0.20 M) in water or acetonitrile. Blank experiments were carried out without catalyst.

Samples of the reaction solution were analysed by GC (chromatograph DANI-86.10; fused silica capillary column 25 m × 0.32 mm × 0.25 μm, CP-WAX52CB, integrator SP-4400, helium as carrier gas), using acetonitrile as an internal standard. The flame ionisation detector response factors were obtained after calibration experiments, using a standard substrate mixture.

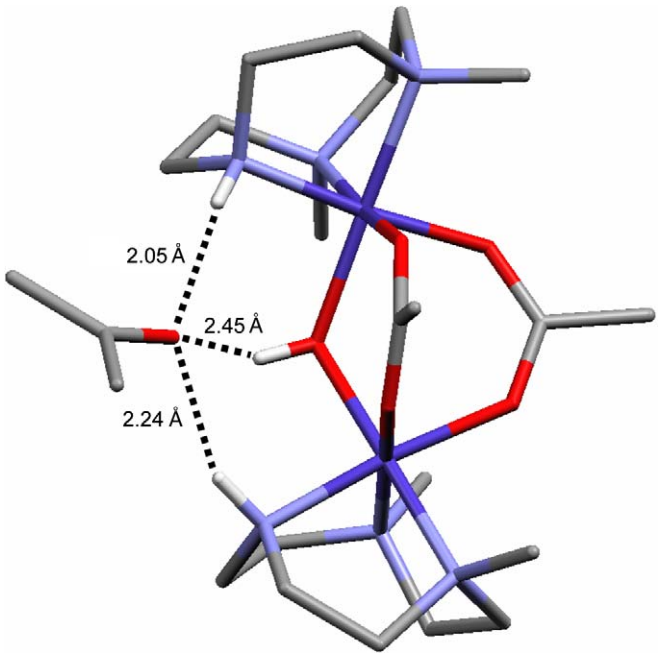

Fig. 4. Capped sticks representation of cation **6** in $[\mathbf{6}][PF_6]_2 \cdot (CH_3)_2CO$, showing the intermolecular interactions with the acetone molecule.

3. Results and discussion

The synthesis of the Fe(III)–Fe(III) complexes, $[L_2Fe_2(O)(OOCCH_3)_2]^{2+}$ and $[(L–Me_3)_2Fe_2(O)(OOCCH_3)_2]^{2+}$, from iron(III) chloride and L or L–Me_3 by a two-step procedure has been described by Wieghardt et al. [3,4]. With the analogous ligand 1,4-dimethyl-1,4,7-triazacyclononane (L–Me_2), we reported recently a simple one-pot synthesis of the Mn(III)–Mn(III) and Mn(III)–Mn(IV) complexes $[(L–Me_2)_2Mn_2(O)_2(OOCH)]^{2+}$, $[(L–Me_2)_2Mn_2(O)_2(OOCCH_3)]^{2+}$, $[(L–Me_2)_2Mn_2(O)(OOCCH_3)_2]^{2+}$ and $[(L–Me_2)_2Mn_2(O)(OOCC_6H_5)_2]^{2+}$ [24]. We now extended this method to the synthesis of $(L–Me_2)_2Fe_2$ complexes containing various carboxylato bridges, in the presence of p-$CH_3C_6H_4SO_3H$ as strong acid and hydrogen peroxide as oxidant, see Scheme 2. Three dinuclear Fe(III)–Fe(III) complexes, $[(L–Me_2)_2Fe_2(O)(OOCH)_2]^{2+}$ (**1**), $[(L–Me_2)_2Fe_2(O)(OOCCH_3)_2]^{2+}$ (**2**) and $[(L–Me_2)_2Fe_2(O)(OOCC_6H_5)_2]^{2+}$ (**3**), have been obtained in moderate to good yields.

All complexes **1**–**3** could be isolated as the hexafluorophosphate salts, which are well soluble in acetone and acetonitrile, but sparingly soluble in ethanol, isopropanol and water. The Fe–O–Fe deformation modes for **2** (725 cm^{-1}) and for **3** (724 cm^{-1}), observed in the infrared spectra, are comparable to those in $[L_2Fe_2(O)(OOCCH_3)_2]^{2+}$ (730 cm^{-1}) [3], whereas for **1** it is shifted to 750 cm^{-1}. In the UV/Vis spectra, the acetonitrile solutions of **1**–**3** show three intense absorption maxima (**1**: 240, 339 and 474 nm; **2**: 230, 341 and 473 nm; **3**: 237, 338 and 476 nm).

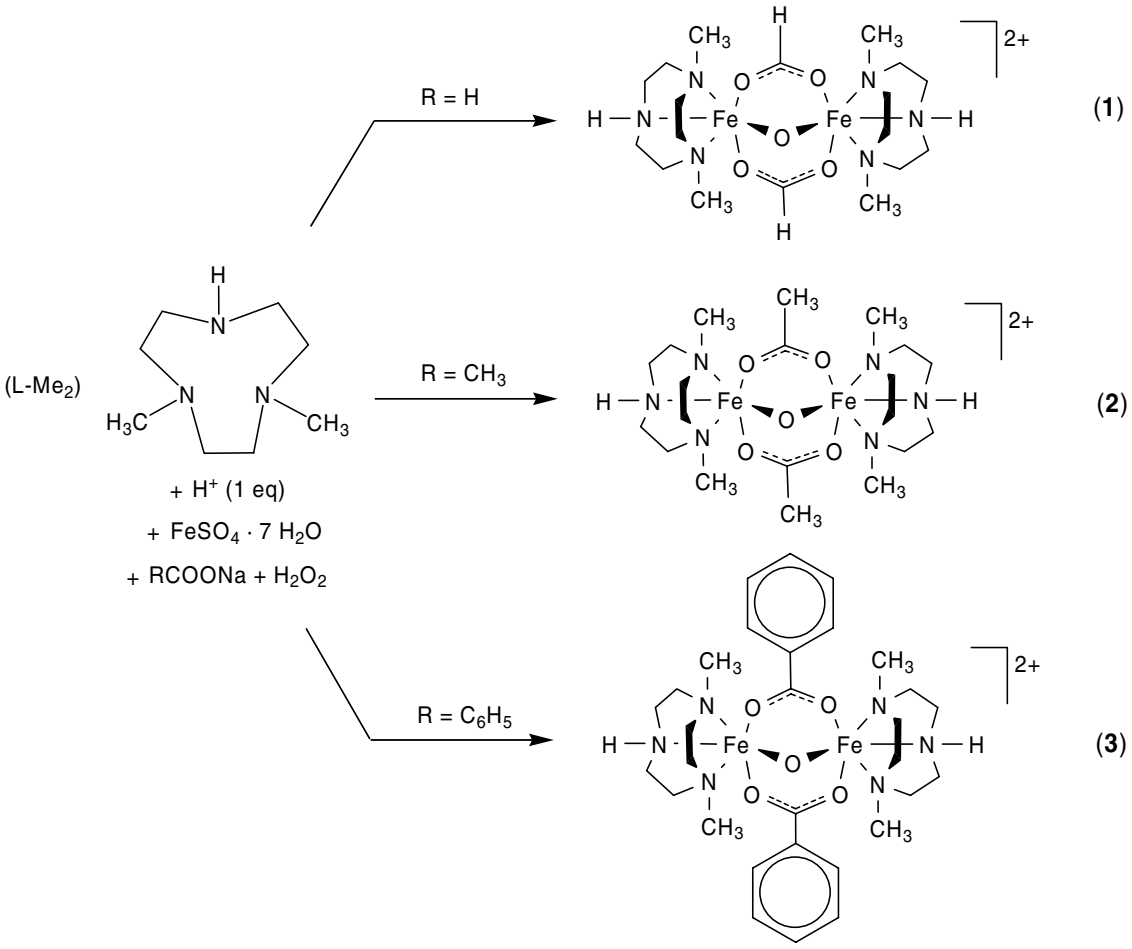

Scheme 2. Reaction of 1,4-dimethyl-1,4,7-triazacyclononane (L–Me_2) with iron(II) sulfate heptahydrate in the presence of hydrogen peroxide and the corresponding sodium carboxylate.

The corresponding reaction with $RuCl_3 \cdot nH_2O$ does not work, however, the analogous Ru(III)–Ru(III) complex $[(L\text{–}Me_2)_2Ru_2(O)(OOCCH_3)_2]^{2+}$ (**5**) can be synthesised by reacting $Ru(dmso)_4Cl_2$ with L–Me_2, HCl and air in refluxing ethanol, followed by addition of sodium acetate (Scheme 3), by analogy to Wieghardt's method for the synthesis of the L–Me_3 derivative [8]. The mononuclear intermediate $(L\text{–}Me_2)RuCl_3 \cdot H_2O$ (**4**) has also been isolated; it precipitates upon addition of water. The ν_{as}(C–O) stretching frequency for **5** at 1559 cm^{-1} as well as ν_s(C–O) frequency at 1428 cm^{-1} are comparable to those in $[(L\text{–}Me_3)_2Ru_2(O)(OOCCH_3)_2]^{2+}$ (1548 cm^{-1} and 1425 cm^{-1}) [7]. The UV/Vis spectrum for **5** shows very intense absorption maxima at 233, 279 and 538 nm, which compare well to those in $[(L\text{–}Me_3)_2Ru_2(O)(OOCCH_3)_2]^{2+}$ [7].

The reaction of L–Me_2, sodium acetate, hydrogen peroxide and triethylamine with $CoCl_2 \cdot 6H_2O$ in acetonitrile yields a dinuclear hydroxo-bridged Co(III)–Co(III) complex $[(L\text{–}Me_2)_2Co_2(OH)(OOCCH_3)_2]^{3+}$ (**6**), see Scheme 4. The presence of the μ-OH bridge is clearly established by a sharp O–H stretching frequency at 3568 cm^{-1}. The ν_{as}(C–O) stretching frequency for **6** at 1590 cm^{-1} is comparable to those of $[(L\text{–}Me_3)_2Co_2(OH)(OOCCH_3)_2]^{3+}$ (1588 cm^{-1}), while the ν_s(C–O) frequency is shifted to higher values (1452 cm^{-1} in **6** versus 1418 cm^{-1} in the known L–Me_3 analogue) [9].

The molecular structures of **2**, **5** and **6**, solved by single-crystal X-ray structure analyses of the hexafluorophosphate salts, are very similar. The two metal centres are linked by two acetato bridges and by an oxo (**2**, **5**) or a hydroxo bridge (**6**), and all metal centres are facially coordinated to a L–Me_2 ligand through the three nitrogen atoms. The single-crystal X-ray structure analyses reveal for the orange crystals of [**2**][PF_6]$_2$ (Fig. 1) a Fe–Fe distance of 3.104(1) Å, for the purple crystals of [**5**][PF_6]$_2$ (Fig. 2) a Ru–Ru distance of 3.230(1) Å, and for the violet crystals of [**6**][PF_6]$_3$ (Fig. 3) a Co–Co distance of 3.358(1) Å. These distances compare well to the isoelectronic Fe(III)–Fe(III) cations $[(L\text{–}Me_3)_2Fe_2(O)(OOCAr^{tol})_2]^{2+}$ [3.114(1) Å, $OOCAr^{tol}$ = 2,6-di(*p*-tolyl)-benzoate] [12], $[(L\text{–}Me_3)_2Fe_2(O)(OOCH_3)_2]^{2+}$ [3.12(4) Å] [4], $[(L\text{–}R_3)_2Fe_2(O)(OOCH_3)_2]^{2+}$ [3.1442(7) Å, R = 3,5-dimethoxybenzyl][25], $[(L\text{–}Me_3)_2Fe_2(O)(OOCCPh_3)_2]^{2+}$ [3.154(2) Å][26], $[(L\text{–}Me_3)_2Fe_2(O)(OOC^tBu)_2]^{2+}$ [3.121(2) Å] [27] and $[(L\text{–}Me_3)_2Fe_2(O)(OOCCH_2C_{10}H_7)_2]^{2+}$ [3.131(1) Å] [28], the Ru(III)–Ru(III) cations $[(1\text{-methylimidazole})_6Ru_2(O)(OOCCH_3)_2]^{2+}$ [3.266(1) Å] [29] and $[(L\text{–}Me_3)_2$-

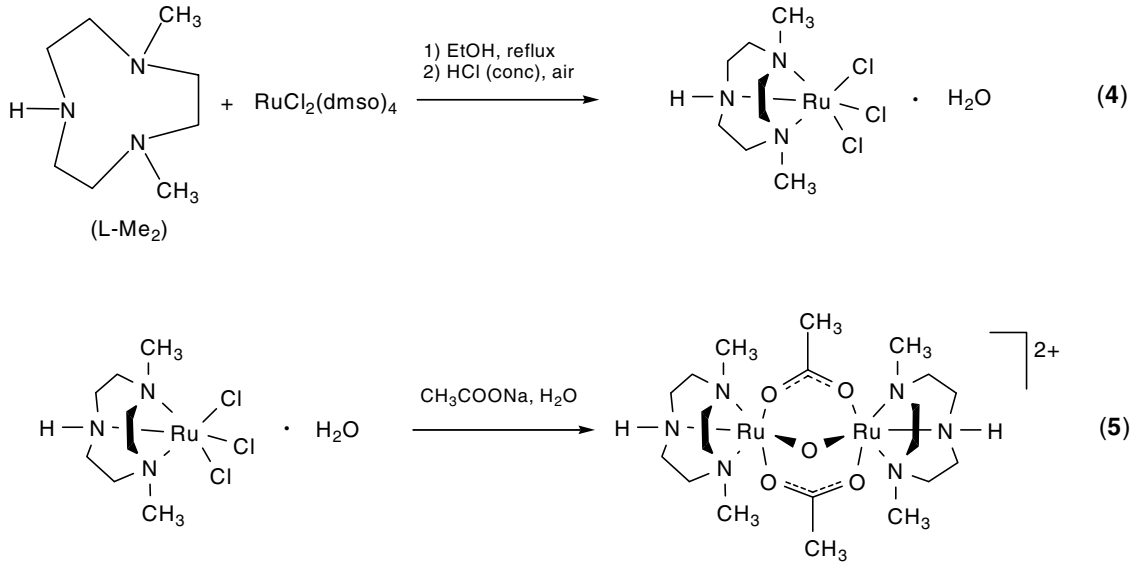

Scheme 3. Reaction of 1,4-dimethyl-1,4,7-triazacyclononane (L–Me_2) with $RuCl_2(dmso)_4$ in the presence of sodium acetate.

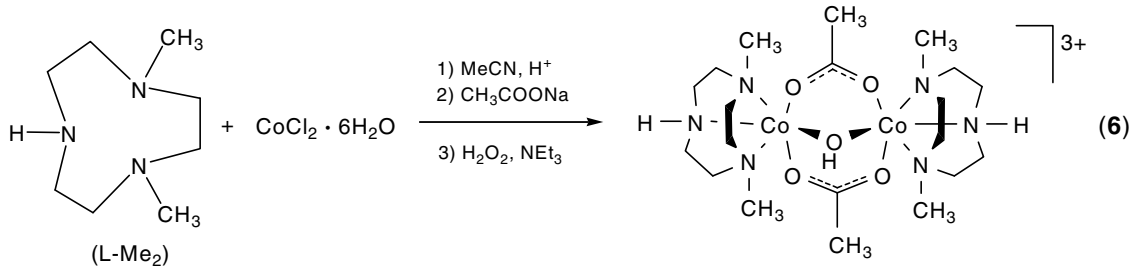

Scheme 4. Reaction of 1,4-dimethyl-1,4,7-triazacyclononane (L–Me_2) with cobalt(II) chloride hexahydrate in the presence of hydrogen peroxide and sodium acetate.

$Ru_2(O)(OOCCH_3)_2]^{2+}$ [3.258(1) Å] [30]; and the Co(II)–Co(III) cation $[(L–Me_3)_2Co_2(OH)(OOCCH_3)_2]^{2+}$ [3.435(4) Å] [9].

Interestingly, all complexes show intermolecular interactions with solvent molecules or anions, owing to the presence of a N–H moiety within the ligand L–Me_2. Therefore, in [**2**][PF_6]$_2$ and [**5**][PF_6]$_2$, the hydrogen atoms of the N–H amino groups interact strongly with the hexafluorophosphate anions. In [**2**][PF_6]$_2$, the distances between the nitrogen atoms and the fluorine atoms of the hexafluorophosphate anion vary from 2.998(7) to 3.285(7) Å with N–H···F angles of 165.3° and 132.3°, respectively, whereas in [**5**][PF_6]$_2$ the N–F distance is 3.234(13) with a N–H···F angle of 159.8°.

In [**6**][PF_6]$_2 \cdot (CH_3)_2CO$, strong hydrogen bonds are formed with an acetone molecule, see Fig. 4. The intermolecular hydrogen bonded system involves the two N–H moieties, as well as the hydroxo bridging ligand. The N···O distances are 2.895(7) and 3.087(8) Å with N–H···O angles of 153.9° and 153.0°, respectively, whereas the O···O distance is 3.080(6) Å with an O–H···O angle of 134.2°.

We tested the catalytic potential of the complexes **1**–**6** for the oxidation of isopropanol with hydrogen peroxide to give acetone, see Scheme 5. The oxidation reaction was carried out in an aqueous solution or acetonitrile in the presence of ascorbic acid at 20 °C. Ascorbic acid was used as a co-catalyst; it may act as a proton donor and as a reducing agent. Reducing agents are obligatory components for oxygenation in most of the biologically active systems [31]. The results are shown in Fig. 5.

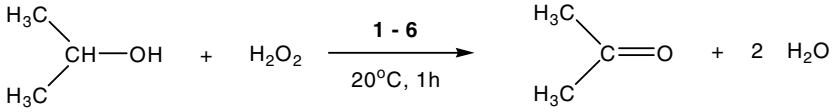

Scheme 5. Catalytic oxidation of isopropanol with hydrogen peroxide.

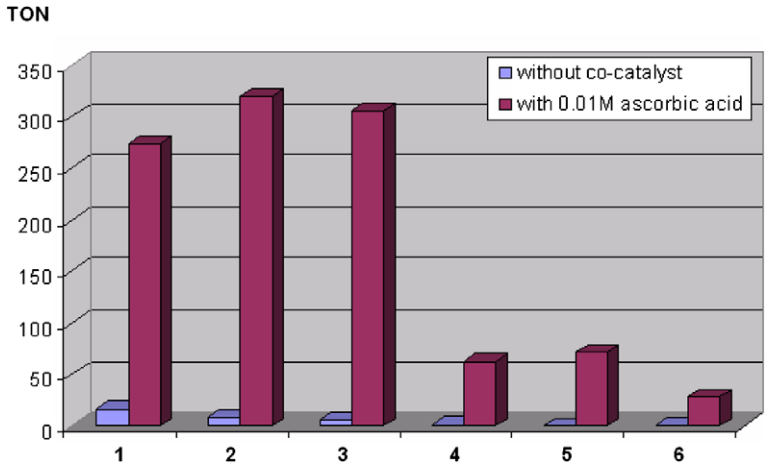

Fig. 5. Oxidation of isopropanol in water, catalysed by the complexes **1**–**6** in the absence/presence of ascorbic acid as co-catalyst (20 °C, 1 h, 1.0×10^{-4} M complex **1**–**6**, 0.20 M isopropanol, 0.50 M H_2O_2, TON – catalyst turnover number).

The highest catalytic activity was observed for $[(L–Me_2)_2Fe_2(O)(OOCCH_3)_2]^{2+}$ (**2**) in the presence of ascorbic acid in water, the TON (catalyst turnover number, mol of products per mol of catalyst) being 320 after 1 h at 20 °C, which is considerably higher than that of the analogous manganese complex $[(L–Me_2)_2Mn_2(O)(OOCCH_3)_2]^{2+}$, for which a TON of 67 was observed under the same conditions [24].

The dinuclear Fe(III)–Fe(III) complexes **1**–**3** can be effectively reduced with ascorbic acid in aqueous solution at room temperature. In the case of $[(L–Me_2)_2Fe_2(O)(OOCCH_3)_2]^{2+}$ (**2**), the intensity of the absorption at 475 nm is reduced by a factor of 10 upon addition of ascorbic acid (Fig. 6), while a new band centred around 590 nm appears with an isosbestic point at 530 nm. By contrast, complexes **4**–**6** are quite stable in the presence of ascorbic acid and thus less active in the oxidation of isopropanol (Table 2). All complexes **1**–**6** in combination with ascorbic acid as co-catalyst are much more active in water than in acetonitrile (Table 2), in line with the complexes $[(L–Me_2)_2Mn_2(O)(OOCCH_3)_2]^{2+}$ and $[(L–Me_2)_2Mn_2(O)(OOCC_6H_5)_2]^{2+}$ in combination with oxalic or ascorbic acid as co-catalyst [24].

Table 2
Oxidation of isopropanol in water and acetonitrile, catalysed by the complexes **1**–**6** in the absence/presence of ascorbic acid as co-catalyst (20 °C, 1 h, 1.0×10^{-4} M $FeCl_2$, complex **1**–**6**, 0.20 M isopropanol, 0.50 M H_2O_2, TON – catalyst turnover number)

Catalyst	TON (after 1 h) in water		TON (after 1 h) in acetonitrile	
	No co-catalyst	With ascorbic acid	No co-catalyst	With ascorbic acid
$FeCl_2$	5	243	2	37
1	17	274	5	29
2	9	320	3	32
3	6	306	3	34
4	2	63	0	5
5	0	72	0	3
6	1	28	0	3

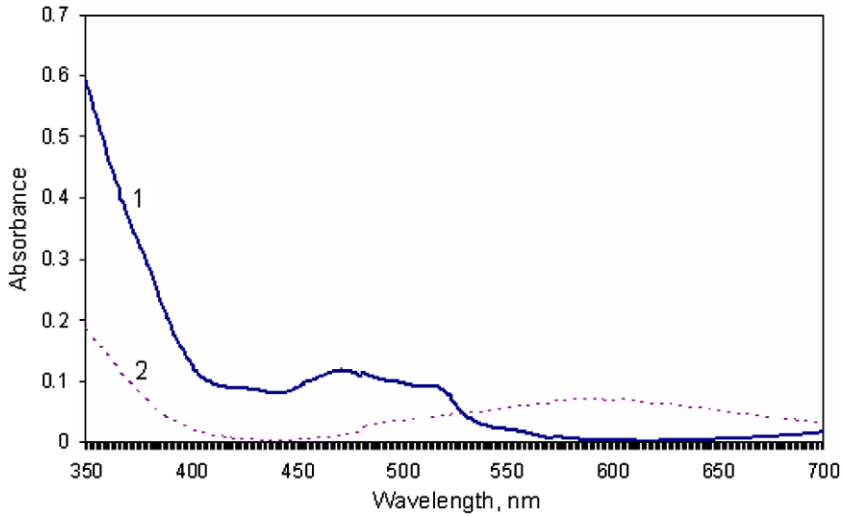

Fig. 6. UV/Vis spectrum of $[(L–Me_2)_2Fe_2(O)(OOCCH_3)_2]^{2+}$ (1.0×10^{-4} M) in the absence (1) and presence (2) of ascorbic acid (1.0×10^{-2} M, 20 °C, 5 min, H_2O).

4. Supplementary materials

CCDC-296748 [**2**][PF_6]$_2$, 296749 [**5**][PF_6]$_2$ and 296750 [**6**][PF_6]$_3 \cdot (CH_3)_2CO$ contain the supplementary crystallographic data for this paper. These data can be obtained free of charge via www.ccdc.cam.ac.uk/data_request/cif, by emailing data_request@ccdc.cam.ac.uk, or by contacting The Cambridge Crystallographic Data Centre, 12, Union Road, Cambridge CB2 1EZ, UK; fax: +44 1223 336033.

Acknowledgements

The authors are grateful to the Fonds National Suisse de la Recherche Scientifique for financial support.

References

[1] A.L. Feig, S.J. Lippard, Chem. Rev. 94 (1994) 759.
[2] L. Que Jr., W.B. Tolman, Angew. Chem., Int. Ed. 41 (2002) 1114.
[3] K. Wieghardt, K. Pohl, W. Gebert, Angew. Chem. 95 (1983) 739.
[4] J.R. Hartman, R.L. Rardin, P. Chaudhuri, K. Pohl, K. Wieghardt, B. Nuber, J. Weiss, G.C. Papaefthymiou, R.B. Frankel, S.J. Lippard, J. Am. Chem. Soc. 109 (1987) 7387.
[5] A.L. Feig, A. Masschelein, A. Bakac, S.J. Lippard, J. Am. Chem. Soc. 119 (1997) 334.
[6] L.D. Slep, A. Mijovilovich, W. Meyer-Klaucke, T. Weyhermüller, E. Bill, E. Bothe, F. Neese, K. Wieghardt, J. Am. Chem. Soc. 125 (2003) 15554.
[7] P. Neubold, K. Wieghardt, B. Nuber, J. Weiss, Inorg. Chem. 28 (1989) 459.
[8] P. Neubold, B.S.P.C. Della Vedova, K. Wieghardt, B. Nuber, J. Weiss, Inorg. Chem. 29 (1990) 3355.
[9] P. Chaudhuri, J. Querbach, K. Wieghardt, B. Nuber, J. Weiss, J. Chem. Soc., Dalton Trans. (1990) 271.
[10] R. Hage, J.E. Iburg, Eur. Pat. Appl. (1993), EP 549271.
[11] R.F. Moreira, E.Y. Tshuva, S.J. Lippard, Inorg. Chem. 43 (2004) 4427.
[12] E.Y. Tshuva, D. Lee, W. Bu, S.J. Lippard, J. Am. Chem. Soc. 124 (2002) 2416.
[13] M. Klopstra, R. Hage, R.M. Kellogg, B.L. Feringa, Tetrahedron Lett. 44 (2003) 4581.
[14] G.B. Shul'pin, G.V. Nizova, Y.N. Kozlov, L. Gonzalez Cuervo, G. Süss-Fink, Adv. Synth. Catal. 346 (2004) 317.
[15] W.-C. Cheng, W.-H. Fung, C.-M. Che, J. Mol. Catal. A 113 (1996) 311.
[16] W.-H. Fung, W.-Y. Yu, C.-M. Che, J. Org. Chem. 63 (1998) 2873.
[17] C. Flassbeck, K. Wieghardt, Z. Anorg. Allg. Chem. 608 (1992) 60.
[18] I.P. Evans, A. Spencer, G. Wilkinson, J. Chem. Soc., Dalton Trans. (1973) 204.
[19] G.M. Sheldrick, SHELXS-97-Program for Crystal Structure Solution, University of Göttingen, Göttingen, Germany, 1997.
[20] G.M. Sheldrick, SHELXL-97-Program for Crystal Structure Refinement, University of Göttingen, Göttingen, Germany, 1997.
[21] A.L. Spek, J. Appl. Crystallogr. 36 (2003) 7.
[22] L.J. Farrugia, J. Appl. Crystallogr. 30 (1997) 565.
[23] I.J. Bruno, J.C. Cole, P.R. Edgington, M. Kessler, C.F. Macrae, P. McCabe, J. Pearson, R. Taylor, Acta Crystallogr. B58 (2002) 389.
[24] V.B. Romakh, B. Therrien, L. Karmazin-Brelot, G. Labat, H. Stoekli-Evans, G.B. Shul'pin, G. Süss-Fink, Inorg. Chim. Acta 359 (2006) 1619.
[25] M. Enomoto, T. Aida, J. Am. Chem. Soc. 124 (2002) 6099.
[26] S.C. Payne, K.S. Hagen, J. Am. Chem. Soc. 122 (2000) 6399.
[27] U. Bossek, H. Hummel, T. Weyhermüller, E. Bili, K. Wieghardt, Angew. Chem., Int. Ed. Engl. 34 (1995) 2642.
[28] L.B. Picraux, B.T. Weldon, J.K. McCusker, Inorg. Chem. 42 (2003) 273.
[29] C. Sudha, S.K. Mandal, A.R. Chakravarty, Inorg. Chem. 32 (1993) 3801.
[30] P. Neubold, K. Wieghardt, B. Nuber, J. Weiss, Angew. Chem., Int. Ed. Engl. 27 (1988) 933.
[31] A.E. Shilov, G.B. Shul'pin, Activation and Catalytic Reactions of Saturated Hydrocarbons in the Presence of Metal Complexes, Kluwer Academic Publishers, Dordrecht, Boston, London, 2000, p. 466.